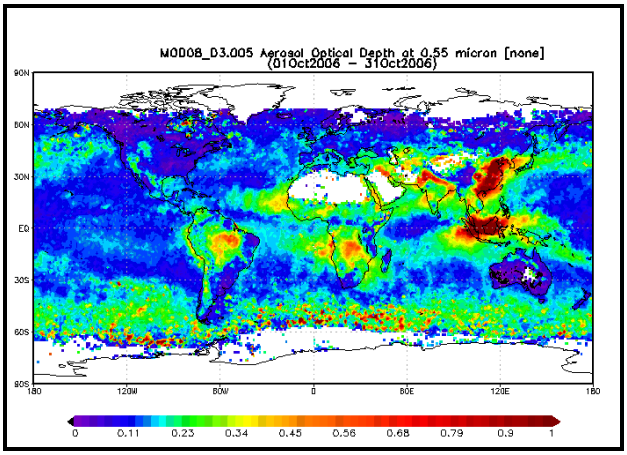

Aerosol Plumes

The cause of

Droughts and El Niño Events

By

Regional Dimming

Keith Potts
Cereal Electricity Pty Ltd
South Australia

Images above from: NASA Goddard Space Flight Centre - Giovanni System[3]
Showing continental scale aerosol plumes: South East Asia and East Asia October 2006; and
The USA Geological Survey showing the eruption of Mount Pinatubo in 1991

Contents

1. Introduction 4
2. Location and Variability of Aerosol Plumes 5
3. The Characteristics of Aerosol Plumes 6
4. The Characteristics of the 2006 Drought in south eastern Australia .. 8
5. Correlations of the 2006 Drought with AOD over the Area 8
6. Conclusions - Recent Australian Droughts 9
7. Drought in Darfur, Sudan 10
8. Australian Droughts from 1890 to 2006 11
9. Volcanic Eruptions and Murray Basin Inflows 13
10. Volcanic Eruptions and the SOI 14
11. Volcanic Eruptions and El Niño 14
12. Correlation and Causation 15
13. The Regional Dimming Model 15
14. Conclusions 17
15. Solution(s) 18
16. References 19
17. Acknowledgements 20
18. Funding Sources 20
19. Tables 21
20. Figure Legends 26

Aerosol Plumes: The cause of droughts and El Niño events by Regional Dimming

Keith A. Potts
Cereal Electricity Pty Ltd
Adelaide, South Australia

Apparitions of seasonal and random anthropogenic, continental scale, aerosol plumes now occur across the globe. Seasonal plumes usually exist for several months and vary significantly in extent and optical depth inter annually. I show that: the aerosol optical depth of the South East Asian Plume correlates with four characteristics of drought in south eastern Australia; the aerosol index of the Middle East Plume correlates negatively with rainfall in Darfur; and the volume of tephra ejected by volcanoes in south east Asia correlates: negatively with rainfall in Australia and water inflows into the Murray River; and positively with ENSO events. I conclude that south eastern Asian aerosol plumes are the cause of drought in south eastern Australia and El Niño/ENSO events and propose a new component of surface aerosol radiative forcing, Regional Dimming, which forces the Inter Tropical Convergence Zone, Hadley and Walker Cells into abnormal seasonal positions causing climate change.

1. Introduction

Anthropogenic aerosol plumes have been studied and reported extensively in the literature. The Intergovernmental Panel on Climate Change (IPCC) Fourth Assessment Report (IPCC Report)[1] identifies two aerosol radiative forcing components, the "Direct Effect" and the "Cloud Albedo Effect" with mean, globally averaged, radiative forcing effects of -0.5 and -0.7 Watts/m^2 and a "Level of Scientific Understanding" (LOSU) of "Medium to Low" and "Low" respectively. Individual aerosol plumes are however reported in the literature to have a surface aerosol radiative forcing (SARF) effect over two orders of magnitude greater than the globally averaged effect reported by the IPCC at -30% and -286 Watts/m^2/τ_α [τ_α being the Aerosol Optical Depth (AOD) of the plume, an open ended scale ranging from 0 crystal clear to 4.5, when the sun would not be visible at noon, and beyond.] The aerosol plumes of interest in this paper exhibit monthly average AOD's over large areas ranging from 0.3 to 1.0 with smaller area daily maxima commonly in excess of 1.0, frequently in excess of 2.0 and rarely in excess of 3.0. Depending on the aerosol types in the plume an AOD of 1.0 with the sun directly overhead could be expected to reduce the direct surface solar radiation (SSR) by ~70% and increase the diffuse SSR by ~30% for a net reduction of surface global SSR of ~20% or more.

The other sources of aerosol plumes relevant to this paper and of similar magnitude to the anthropogenic plumes are volcanoes and, as an extreme example, the Mount Pinatubo eruption in 1991 ejected an estimated 11 Km^3 of tephra into the atmosphere which was still detectable over two years after the eruption. Tephra is defined by the United States Geological Survey as "… fragments of volcanic rock and lava regardless of size that are blasted into the air by explosions or carried upward by hot gases in eruption columns".

The IPCC Report[2] also provides comments on recent extreme weather events and, in reference to the August 2003 heat wave in Europe, states: "The 2003 heat wave was associated with a very robust and persistent blocking high-pressure system that may be a manifestation of an exceptional northward extension of the Hadley Cell".

This paper identifies a new aerosol component of climate change, Regional Dimming, caused by apparitions of continental scale, optically dense, anthropogenic and/or volcanic, aerosol plumes in the tropics which exhibit SARF effects over two orders of magnitude greater than the averaged SARF recorded in the IPCC Report. Regional Dimming and its effects are a direct result of the highly inhomogeneous and temporally variable nature of the global aerosol coverage and these effects are lost when the aerosol coverage is globally averaged in time or space in climate modelling. The Regional Dimming Model (RDM) is proposed to explain how "persistent, blocking high-pressure systems" are produced as exceptional extensions of the Hadley Cells in both the northern and southern hemispheres.

Some continental scale, tropical aerosol plumes exhibit strong seasonality, existing during the same months each year, and, as they have increased in optical depth and geographic extent over recent decades due to increasing populations, industry and tropical agriculture, their

effect on the regional and global climate has also increased and, appearing at the same time each year with the same effects, they are causing significant climate change.

The data sets used in this analysis were either purchased from the Australian Bureau of Meteorology (ABOM) or downloaded from free sources and were processed into time series of monthly and annual averages. The data sets were then correlated to demonstrate that both anthropogenic and volcanic aerosol plumes of continental scale have an immediate, significant effect on both the regional and global climate.

2. Location and Variability of Aerosol Plumes

The global aerosol coverage is highly inhomogeneous and varies significantly through the year with dense, continental scale plumes occurring at different times and in different locations as can be seen in the two images in Figure 1 from the NASA MODIS Giovanni System (NMGS)[3].

Five such aerosol plumes are identified in the images in Figure 1:

The **South East Asian Plume** centred over Sumatra and Borneo in the October 2006 image. This anthropogenic seasonal plume originates from biomass combustion from tropical agriculture with significant increases due to rainforest clearing in 1997-98, 2002 and 2006;

The **Central American Plume** over southern Mexico in the May 2005 image is probably a volcanic eruption;

The **South American Plume** covering the Amazon basin in northern South America in the October 2006 image. This anthropogenic seasonal plume has similar origins to the South East Asian Plume – tropical agriculture and rainforest clearing.

The **East Asian Plume** covering the eastern Asian seaboard from latitude 20N to 40N in the October 2006 image is another anthropogenic plume and originates from increasing levels of agriculture and industrialisation. This plume varies throughout the year but can be clearly identified during all months of the year.

The **Middle East Plume**, an anthropogenic aerosol plume which can be seen over the Red Sea, Persian Gulf and north west Indian Ocean in the May 2005 image. Data from desert and ice covered areas is masked in the NMGS for technical reasons and is therefore not available for much of the Middle East and Sahara Desert.

Each apparition of the seasonal anthropogenic plumes typically lasts for several months and recurs at the same time each year. For example the South East Asian Plume is visible each year on the available NMGS images and typically erupts in July, peaks in September/October and collapses in November with the start of the South East Asian monsoon. All such plumes exhibit significant inter-annual variability and two apparitions of the South East Asian Plume

in October 2005 and 2006 in the NMGS Images in Figure 2 demonstrate this. It is clear from these images that the South East Asian Plume was much larger and more optically dense in October 2006 than in 2005 and this is confirmed in Figure 3 which shows the average AOD from the NMGS plotted for the area covered by the plume from latitude 10^o S to 10^o N and from longitude 90^o E to 160^o E (the Area) with an average AOD of 0.45 in October 2006 compared with 0.16 in October 2005.

3. The Characteristics of Aerosol Plumes

In the literature dense, continental scale, aerosol plumes are reported to have a very large SARF with reported measurements and estimates at -30%, -172 W/m^2 and -286.0 W/m^2/τ_α which are more than two orders of magnitude greater than the SARF shown in the IPCC Report after global averaging at -0.7 and -0.5 W/m^2. Four references from the literature are provided for the SARF effect of such aerosol plumes:

Ramanathan[4] reports the reduction of Photosynthetically Active Radiation (PAR) reaching the earth's surface under aerosol plumes in the Indian Ocean as: "The brown clouds over the Arabian Sea decreased direct PAR by 40% to 70%, but enhanced the diffuse PAR substantially, with a net reduction in total PAR by as much 10% to 30%."

Mitchell et al[5] report that during the 2003 bushfires in Canberra, Australia, the aerosol plume: ".. gave rise to mean radiative forcings of -50 W m^{-2} at the top of the atmosphere and -172 W m^{-2} at the surface…"

Duncan et al[6] report that the Indonesian fires of 1997-98 gave rise to significant radiative forcings: "The net direct, shortwave radiative forcing at the top of the atmosphere of OC and BC aerosols from the fires was relatively small, as their forcings were similar, but of opposite signs. The net forcing at the surface, however, was large, about −10 W m^{-2} over most of the tropical Indian Ocean and as low as −150 W m^{-2} over the burning regions in Indonesia, indicating that aerosols from the fires significantly perturbed the tropical radiative budget."

Hansell et al[7] reporting on surface radiative forcing efficiency state that: "The retrieved aerosol optical depths were then used along with the total surface flux measurements to derive the forcing efficiencies for different air-mass intervals on the basis of linear least-squares fitting. The larger efficiencies found for SAFARI [~-176.0(W/ m^2)/τ_α] and ACE-Asia [~-286.0(W/ m^2)/τ_α] are most likely due to the highly absorbing aerosols generated from local biomass burnings, biological and industrial sources, and urbanized sources."

The WMO Radiation Database[8] includes data for Singapore Airport. Figure 4 shows the mean monthly solar radiation data for 1997 with the "direct", "diffuse" and "global" radiation plotted on the left axis and the number of Indonesian fires[9] plotted on the right hand axis. The changes in surface radiation are shown in Table 1.

When an aerosol plume, such as the South East Asian Plume, is located over the ocean, the level of SARF described above will affect the Sea Surface Temperature (SST) and produce localised cooling under the plume. This can be seen clearly in Figure 5 where the SST anomaly map from the Australian Bureau of Meteorology Research Centre[10] for the week ending 15th October 2006 is shown in the left image and the NMGS mean AOD for October 2006 in the right image. The correlation between the aerosol plume and the SST anomaly around Indonesia and under the south east trending aerosol plume from south eastern Asia towards the southern tip of South America is clear.

SST mean monthly data for the Area was downloaded from the National Oceanic and Atmospheric Administration (NOAA) website[11] and correlated with the NMGS AOD data for the Area. The results are shown in Table 2. The correlation coefficient R, number of samples N, significance level *P* using the two tailed test, and R^2, are shown in this and all subsequent correlation tables.

It is noted here that analysis using correlation coefficients demonstrates association, not causation, and that the relationships discussed in this paper may not necessarily be simple or linear. The issue of causation is discussed later.

A scatter plot of mean AOD and SST for the months of August to November from 2000 to 2007 is shown at Figure 6 together with the linear trend line for each month. Figure 6 and Table 2 demonstrate a clear negative relationship between SST and AOD in the Area.

Mitchell et al[5] report that the smoke plume emanating from the Canberra bush fires in Australia in 2003 reduced the forecast wind speed significantly and provided Table 3 of actual and forecast wind speeds showing a significant reduction in actual wind speed versus forecast:

> "The smoke layer that blanketed the Canberra region in the week following the fires can explain the suppression of maximum surface temperatures and wind speeds relative to forecasts. This occurred due to the stabilizing effect of the plume, inhibiting convection in the boundary layer through a marked reduction in surface heating, and stabilizing the lower part of the smoke layer by setting up a positive gradient in heating rate. These changes reduced the fire risk during this period, in one case contrary to a forecast of renewed fire danger with significant economic consequences. This suggests a case for the inclusion of aerosol effects in fire weather prediction models."

Aerosol plumes such as the South East Asian Plume are therefore reported to:

- Produce very large SARF effects; and
- Suppress the winds.

4. The Characteristics of the 2006 Drought in south eastern Australia

South eastern Australia suffered one of the worst droughts on record in 2006 as the graphs in Figure 7 with data from the ABOM demonstrate. The absence of rain in October 2006 is particularly striking in both graphs in Figure 7 and in the August to November period the Riverina West Rainfall District (RWRD) received only 36% of its average rainfall for this period.

Coincident with the drought was a persistent, high pressure system over south eastern Australia which was much further south than is normal at this time of year. An example is shown in the MSL Analysis chart in Figure 8 from the ABOM[12]. The MSL pressure anomaly map for October 2006 on the ABOM web site shows a +7 hPa mean sea level pressure anomaly over most of Victoria and +6 hPa over most of south eastern Australia. This high pressure system is interpreted to be an exceptional southward extension of the southern Hadley Cell, being over ten degrees of latitude further south than the high pressure ridge at the western edge of Figure 8 which is the southern extremity of the southern Hadley Cell over the Indian Ocean.

The atmospheric moisture levels in south eastern Australia were also anomalously low and in October 2006 the average dew point at Swan Hill airport in Victoria, on the south west border of the RWRD, was $+1.9^{o}$ compared with an average for October of $+5.8^{o}$ and is, in fact, the lowest average dew point on record for the month of October in Swan Hill.

The average SST of the Area was the lowest recorded in September, October and November 2006 compared with other years from 2000 to 2007

The characteristics of the 2006 drought in south eastern Australia in 2006 were therefore: significantly reduced rainfall (obviously); very low dew point/humidity; a positive MSL pressure anomaly over the south east of the continent; and historically low SST's in the Area. These characteristics will be demonstrated to correlate with the Aerosol Optical depth ("AOD"), of the South East Asian Plume over the period for which common data is available: 2000 to 2006/7.

5. Correlations of the 2006 Drought with AOD over the Area

Correlations of AOD averaged over the Area, and rainfall in the RWRD in south eastern Australia from August to November using data for the period 2000 to 2006, are listed in Table 4. The correlation for October is particularly striking. Figure 9 is a scatter diagram of rainfall in the RWRD and the monthly average NMGS AOD over the Area. The trend lines for each month from August to November are negative reflecting the fact that the higher AOD levels of the South East Asian Plume correlate with lower rainfall in the RWRD during these months.

Correlations of aerosol optical depth ("AOD"), averaged over the Area, and the ABOM 9:00am MSL pressure for Melbourne Airport are shown in Table 5. Data for Melbourne Airport is used here as this site is close to the centre of the anomalous high pressure system in Figure 8 and again the October correlation is seen to be statistically significant. A scatter plot of this data together with trend lines for each month is shown at Figure 10. The linear trend lines in all months are positive showing that increasing AOD of the South East Asian Plume correlates with increasing MSL pressure in Melbourne during this period.

As shown above the South East Asian Plume cools the sea surface by SARF. The Australian Bureau of Meteorology has stated that:

> "Moreover, Australia's climate may continue, at least in the short term, to be influenced by the unusual state of the oceans to the north, and particularly northwest, of the continent. These have been cooling strongly since June when, historically, they would have been expected to warm as other indicators became more La Niña-like. This pattern inhibits the formation of northwest cloudbands, which are a major source of winter and spring rain for central and southeastern Australia during La Niña years."[13]

It must therefore be expected that there will be a correlation between the AOD of the South East Asian Plume over the Area and humidity in south eastern Australia and this will demonstrate that the third characteristic of the 2006 drought is linked to the South East Asian Plume. Since humidity data is not provided on the Bureau of Meteorology data CD the 9:00am dew point is used as a proxy for humidity and Swan Hill airport is the station used. The correlations for 2000 to 2006 are shown in Table 6 and the scatter plot for the two parameters in Figure 11.

Table 6 shows statistically significant negative correlations from August to October demonstrating that a higher AOD in the Area correlates with a lower dew point and hence lower humidity in Swan Hill during this period.

6. Conclusions - Recent Australian Droughts

Table 7 shows the statistically significant correlations between the South East Asian Plume and the main characteristics of the 2006 drought in south eastern Australia. Significance <0.05 is shown in green and <0.01 is shown in yellow. The high correlations in October across all characteristics reflect the facts that: the South East Asian Plume is at its most intense during this month; and this is also the month when the ITCZ would normally be transiting the latitudes covered by the plume, 10^{o}N to 10^{o}S. November is included above to demonstrate that the effect reduces in this month with the start of the south eastern Asian monsoon early in the month. This extinguishes the South East Asian Plume. Hence the South East Asian Plume creates drought in south eastern Australia in two reinforcing ways:

Firstly by cooling the sea surface in the Area which reduces evaporation and thereby reduces the moisture levels in the atmosphere in south eastern Australia;

Secondly by creating an anomalous, persistent high pressure system over southern New South Wales and Victoria which forces the low pressure systems on the Antarctic front further to the south and reduces the number of cold fronts, which are major trigger events for rain, crossing south eastern Australia.

Thus the South East Asian Plume reduces both the number of rainfall events and the amount of rain received from each event in south eastern Australia and creates drought.

It should also be noted that this is a simple analysis of a complex system with: The ITCZ traversing from the northern tropics in July/August to northern Australia in November; The South East Asian Plume exhibiting significant variation in AOD and geographical extent; and the effect of the East Asian Plume in combination with the South East Asian Plume being ignored.

Even with this caveat the statistically significant correlations in October between the South East Asian Plume and the characteristics of the 2006 drought in south eastern Australia and other statistically significant correlations in August, September and November force the conclusion that the South East Asian Plume is responsible for recent droughts in south eastern Australia. However this leaves open the question of historic droughts in south eastern Australia which occurred before the South East Asian Plume existed in its current form and this issue is addressed later.

7. Drought in Darfur, Sudan

Darfur, in western Sudan, lies approximately within the area bounded by latitude 11^{o}N to18^{o}N and longitude 23^{o}E to 28^{o}E. Rainfall in Darfur is highly seasonal with 93% falling in May to September and 60% in July and August alone. The Sudan Meteorological Authority states on its report for the period 21 to 31 August 2004: “Rainfall in Sudan and its seasonal distribution is mostly the result of the northwards movement of moist air masses, source of the rainfall. The Intertropical Convergence Zone (ITCZ) marks the northernmost extent of these humid air masses, where they meet with drier and warmer air. The rains follow some distance south of this border between air masses, so that tracking this ITCZ through the season provides a quick evaluation of the seasonal movement of the rains”.

Regional Dimming to the south of Darfur would therefore be expected to show a significant negative correlation with rainfall in Darfur if the Middle East Plume, as reported by Mitchell et al[5], suppresses the winds and the movement of the humid air masses into Darfur from the south. Rainfall data for Darfur was downloaded from the NASA Giovanni Global Precipitation Climatology Project (NGGPCP) rainfall analysis tool[14]. Aerosol Index (AI) data was downloaded from the NASA Giovanni TOMS system (NGTS) [15] using the area latitude

9^oN to 11^oN and longitude 23^oE to 28^oE (Area D). The years of available common data are 1979 to 1992.

The correlations of rainfall in Darfur and the AI for Area D for the months of May to September are shown in Table 8. Rainfall in other months is so low (<15mm average) that those months are not included. July and August show statistically significant correlations. A scatter plot of the data for May to September is shown in Figure 12. Two images of AI for the month of August 1990 are shown in Figure 13. The left image using a palette extending from 0 to 1 shows the geographic extent of the aerosol plume and the right image with a palette from 1 to 4.5 shows the sources of the aerosols.

Figure 14 shows the AI of Area D plotted against rainfall for the month of August. The years 1987, 88 and 89 are particularly interesting showing a dramatic, close, negative relationship between rainfall in Darfur and AI over Area D.

These correlations demonstrate that, in a totally different context to the Australian droughts, aerosols again correlate with drought. In this case by suppressing the moist southerly winds the Middle East Plume prevents the ITCZ moving north in Sudan and causes drought in Darfur.

8. Australian Droughts from 1890 to 2006

South eastern Australia suffered from droughts long before the anthropogenic South East Asian Plume, emanating from tropical agriculture and rainforest clearing, existed at a sufficient scale to affect the climate in Australia. A proposal that the cause of recent droughts in south eastern Australia is the anthropogenic South East Asian Plume must therefore provide an explanation for these historic droughts.

Volcanoes are a major source of aerosol plumes and have the ability to create aerosol plumes which are as, or more, extensive and of similar AOD compared with the South East Asian Plume. The volcanoes in the region are shown in Figure 15 from Google Earth[16] with the Smithsonian Institution (SI) volcano overlay[17]. Each small red triangle is one volcano. The Area used for aerosol averaging for the South East Asian Plume in the previous discussion is shown in pale green and contains a significant number of volcanoes.

Therefore if the Regional Dimming Effect is in fact the cause of drought in south eastern Australia, a negative correlation would be expected between volcanic eruptions in the Area and rainfall in south eastern Australia. Volcanic eruption data is available on the SI web site and the SI provided a spreadsheet version of the volcanic eruption database for the period 1800 to 2006[17]. This database includes:

The year, month and day of the start of the eruption with some eruptions only recording the year and some only the year and the month;

The year, month and day of the end of the eruption with the same caveats as the start date;

The Volcano Explosivity Index ("VEI"), a "near logarithmic" scale which records the size of the eruption and ranges from: "0" described as "Effusive"; to "6" for "Pinatubo" in 1991 and is open ended. Super Volcanoes such as that under Yellowstone National Park would be an "8" on this scale. 5072 out of 5526 eruptions (92%) are recorded with a VEI. Eruptions without a VEI were set to a VEI of "0" during processing

The estimated volume of tephra ejected into the atmosphere is recorded for 432 of the 5526 eruptions (8%) in the database. Tephra is measured in cubic metres as 10^x and the figure included in the database is "x". Hence for each unit increase in "x" the volume of tephra increases by a factor of 10. The figure provided is an estimate and, as an example, the volume of tephra ejected by Mount Pinatubo is stated to be "$1.1 \pm 0.5 \times 10^{10}$ m^3" or between 6 and 16 cubic kilometres – a significant range.

All volcanic eruptions were allocated a start date either from the data available in the database or by allocating "1" to missing months and days for the period 1800 to 2006. Hence an eruption with only the year in the start date was allocated 1st January of that year as the start date and an eruption with only the year and month in the database was allocated the 1st of that month as a start date. The volcano database was then modified to enable the selection of volcanoes in a specific geographic area and month or series of months. In this study volcanoes were selected from within the Area.

The database was then processed to select eruptions from 1st April to 31st October inclusive each year to coincide with the wet season in south eastern Australia when the majority of the rainfall is received (63% in the Riverina West Rainfall District and 79% in Adelaide). The volume of tephra recorded in the database as ejected by these volcanoes in these months was summed for each year and then correlated with the rainfall in the Riverina West rainfall district in column A including all years and in column B including only years with reported tephra for the period 1890 to 2006. The results of these correlations are shown in Table 9 and the scatter plot of all the data is shown in Figure 16.

These correlations demonstrate a statistically significant negative correlation between recorded tephra and rainfall in the RWRD and the linear trend shows that on average in a year with 0.1 Km^3 of tephra ejected by the volcanoes in the Area between April and October the RWRD can expect to experience a 31% reduction in rainfall from 242mm (no tephra) to 168mm.

Since only 8% of the volcanic eruptions in the SI database record the volume of tephra ejected, this data was viewed as incomplete and the VEI data covering 92% of the eruptions since 1800 was converted to tephra using the table available at the SI Global Volcanism Program website[18]. Selecting the same geographic area and months for the period 1890 to 2006

the "VEI to tephra data" was correlated with rainfall in the Riverina West Rainfall District. The resulting correlations and confidence levels are shown in Table 10. A scatter plot of the data is shown in Figure 17.

It can be clearly seen from both the volcanic tephra and VEI to tephra data that a statistically significant, negative correlation exists between tephra ejected by volcanoes in the Area and rainfall in the RWRD of south eastern Australia. Averaging the linear trend line slopes on the scatter plots gives an average reduction in rainfall in the RWRD of 63.2 mm for the April to October period for each 0.1 cubic kilometres of tephra ejected by the volcanoes in the Area in the same period.

9. Volcanic Eruptions and Murray Basin Inflows

The Murray River is the major water source for much of south eastern Australia and is a source of extreme concern in 2008 as the inflows to the river system were at the lowest levels on record in 2006/07. The Murray Darling Basin Commission (MDBC) stated in its December 2007 Drought Update No 11 that: "Inflows over the 2006/07 water year were just 55% of the previous minimum on record." Data on the "total water inflows to the Murray System - including Menindee" was provided by the MDBC[19] for the years 1891 to 2007 with the following caveat, "Please note that these figures include modelled data and are subject to change - they should be viewed as indicative only".

This data was processed to give inflows for the months April to October each year and correlated with the "VEI to Tephra" data for volcanic eruptions for the same months from 1892 to 2006. The correlation table is shown in Table 11 with a significance level of 0.1. The scatter plot is shown in Figure 18 which shows data for all the years with a linear trend line and the equation for the trend line showing that for every 1/10 Km^3 increase in the eruption of tephra in the Area the water inflow into the Murray River reduces by 3,127 GLt on average.

Both these datasets have to be treated with caution. The Murray River inflow data comes with the caveat quoted above. The VEI allocated to an eruption used in this analysis is accompanied by a "?" in 94 of the 935 cases (10.05%) and no VEI is allocated to 8% of the eruptions. The SI's web site describes the "?"as:

> "A "**?**" accompanies those VEIs that were particularly difficult to assign, and those that are based on purely circumstantial evidence. For example, a VEI of 1? might have been assigned to an undescribed eruption because a nearby contemporaneous eruption received sufficient historical comment to confidently assign a VEI of 2. When there was simply no evidence on which to base a VEI, this column has normally been left empty (20% of the eruptions in our file)."

In these circumstances an averaging process will reduce the noise in the data. The "VEI to Tephra" falls naturally into several bands due to the allocation of integer VEI's only to each eruption. Hence the data was segmented into six "VEI to Tephra" bands of: Less than 0.001Km^3; 0.001 to 0.01 Km^3; 0.01 to 0.02 Km^3; 0.02 to 0.1 Km^3; 0.1 to 0.2 Km^3; and greater than 0.2 Km^3 and the inflows to the Murray River were averaged for the years falling into each band. The correlation of this averaged data is shown in Table 12 and the scatter plot of the data is shown in Figure 19 with a "power" trend line.

The conclusion from this analysis is clear. Increased levels of tephra ejected by volcanic eruptions in the Area cause reduced water inflows into the River Murray in the April to October period.

10. Volcanic Eruptions and the SOI

Drought in south eastern Australia is commonly accepted as correlating with ENSO (El Niño /Southern Oscillation Index ("SOI")) events and, as we have seen that rainfall in south eastern Australia and Murray River inflows are negatively correlated with aerosols from the South East Asian Plume and volcanic tephra, we should expect to find a relationship between volcanic eruptions and ENSO events.

The SOI data was downloaded from the Australian Bureau of Meteorology web site[12], averaged for each year and plotted against the total "VEI to Tephra" for each year with all months included for the period 1891 to 2006. Two scatter plots of the SOI and "VEI to Tephra" are provided in Figure 20. The left graph shows all years with a linear trend line and the right graph shows the data segmented and averaged into seven bands.

The correlations for the segmented and averaged SOI and "VEI to Tephra" data are shown in Table 13. Column A shows all years and column B shows all years except 1963 when a major eruption of the volcano Agung commenced in February and ejected more than 1 Km^3 of tephra into the atmosphere. This was by far the largest eruption event in the study period.

This data demonstrates a clear statistically significant relationship between the SOI and volcanic eruptions in the Area when the sole, extremely large volcanic eruption is excluded from the analysis and it should be noted that the relationship only shows a positive average SOI for years with a total tephra volume erupted from the Area which is less than 0.03 Km^3.

11. Volcanic Eruptions and El Niño

One of the main characteristic of El Niño events is an increase in the Sea Surface Temperature ("SST") in the Niño regions. In this study the SST anomalies for Niño region 3.4 were downloaded from the web site of the Climate Analysis section at the National Center for Atmospheric Research (NCAR) in Boulder Colorado[20].

This SST data was then correlated with the "VEI to Tephra" data derived from the SI database. The correlations of the data are shown in Table 14. Column A includes data from all years from 1891 to 1999 and column B excludes 1963 for the reason previously stated. The scatter plots are shown in Figure 21, all years (L), and segmented and averaged (R).

This data shows a clear positive relationship between volcanic eruptions in the Area and the SST anomalies in the Niño 3.4 region, latitude 5^{o}N to 5^{o}S and longitude 170^{o}W to 120^{o}W.

12. Correlation and Causation

It is a well known scientific fact that "correlation does not imply causation" and if two events A and B correlate there are five options to explain the relationship:

1. A causes B;
2. B causes A;
3. C, another event, causes A and B simultaneously;
4. It's a coincidence;
5. There is a complex relationship involving feedback.

Then if A = "volcanic eruptions in the Area" and B = "Murray River Inflows" options 2, 3 and 5 above are impossible since deep earth processes cause volcanoes to erupt and inflows into the Murray River cannot cause volcanic eruptions in the Area or indeed anywhere. This leaves options 1 and 4 and either the volcanic eruptions are causing the reduction in inflows to the Murray River or it's a coincidence. With the same logic applying to the correlations of volcanic eruptions with the SOI, Niño 3.4 SST and RWRD rainfall the weight of evidence is against coincidence and the only logically valid conclusion which can be drawn from this analysis is that volcanic eruptions in the Area caused the ENSO events and droughts in south eastern Australia over the last century.

The similarity of the South East Asian Plume to the tephra plumes from volcanic eruptions along with similar reasoning on the correlations must therefore force the conclusion that the South East Asian Plume has been the cause of recent drought in south eastern Australia.

13. The Regional Dimming Model

The Regional Dimming Model (RDM) is proposed to demonstrate how such aerosol plumes affect the climate in both the region of the plume and in the higher latitudes. The analysis, without access to a global circulation model ("GCM"), is, of necessity, simple. The RDM is described using a SARF of -20% based on the published literature cited above.

In Figure 22 the sun is assumed to be over the equator and the graph shows the level of surface solar irradiance relative to that received at the equator plotted against latitude for both hemispheres. Values range from 100% at the equator to zero at the poles. Under these conditions and ignoring the lag between the sun's position and the ITCZ position, the ITCZ will be at the equator as marked and the Hadley Cells will extend from the equator to about 30^o N latitude and to 30^o S latitude.

Figure 23 shows the same conditions with the addition of an aerosol plume extending from 10^o N to 10^o S latitude with a constant surface radiative forcing effect of -20%. Under these conditions it is clear that the maximum surface solar irradiance is not at the equator but at the edges of the plume. This will split the ITCZ and create two ITCZ's at the northern and southern edges of the plume, one at 10^o N latitude and one at 10^o S latitude. This splitting and movement of the ITCZ to abnormal seasonal positions will, in turn, move the Hadley Cells from their normal positions described above to positions which extend to 40^o N and to 40^o S latitude.

Such an aerosol plume will also suppress the winds as described by Mitchell et al. In this case the winds are the Trade Winds and the suppression of them in the area of the plume must exclude the ITCZ from the area of the plume as it is the convergence of the north east and south east Trade Winds which forms the ITCZ.

It should also be noted that this change of 10 degrees of latitude in the position of the regional Hadley Cell will produce a persistent, blocking, regional, high pressure cell as an "exceptional extension of the Hadley Cell" and, since the cause of the atmospheric circulation perturbation is regional and static, the effect will also be regional and static. The RDM can therefore produce the effect described in the IPCC Report with reference to the August 2003 heat wave in Europe and seen during the 2006 drought in south eastern Australia.

Extending this analysis from the general to the particular it is clear that, with the South East Asian Plume in place from July to November, the ITCZ will split and the southern ITCZ will control the position of the regional, southern Hadley Cell which will be forced to an abnormally southerly position during the period and result in an anomalous persistent high pressure system over the south east of Australia which, as we have seen, contributes to the drought in that region. Under these circumstances the RDM will produce a summer atmospheric circulation system in the Australian region whilst the sun is overhead the northern hemisphere, in effect an Australian "summer-in-winter".

As the Hadley Cells are linked with the Walker Cell over south eastern Asia, moving the Hadley Cells to abnormal seasonal positions will also result in the Walker Cell moving to an abnormal position and this will reduce the wind speed in the Niño 3.4 area which in turn will cause an increase in the SST in that area – an El Niño.

The effects of the South East Asian Plume on the scalar wind speed derived from the NCEP/NCAR reanalysis data[21 22] can be seen in Figure 24 where the wind speeds for August to November for the three years (2000, 2001 and 2005) with the lowest October AOD in the Area are deducted from the three years (2002, 2004 and 2006) with the highest October AOD in the Area in the period 2000 to 2006 to show the anomalies caused by the Plume. The wind speed over the Niño 3.4 area reduces across the area by up to 1m/s. A reduction in wind speed over south eastern Australia can also be seen as well as an increase in wind speed to the south of the continent as the low pressure systems with higher wind speeds are forced south by the anomalous southerly extension of the Hadley Cell.

Therefore the Regional Dimming Theory is stated as:

> **Optically dense aerosol plumes in the tropics interfere with the seasonal movement of the ITCZ. Depending on their optical depth, size and location such plumes may either split the ITCZ into northern and southern components separated by many degrees of latitude or stop the seasonal movement of the ITCZ. These effects move the southern and northern Hadley Cells and consequently the entire atmospheric circulation system in the region of the aerosol plume into abnormal seasonal positions. This causes significant climate change near the longitudes of the plume in the tropics, by modifying the local wind systems. In the higher latitude regions remote from the aerosol plume the plumes create persistent, blocking, high pressure systems as abnormal extensions of the Hadley Cells and can also, in some regions, reduce the amount of water vapour in the atmosphere by cooling the sea surface. If the aerosol plume extends beyond the tropics, one component of the ITCZ may even be forced outside the tropics resulting in extremely anomalous conditions in the higher latitudes. The South East Asian Plume, by interfering with the movement of the ITCZ and Hadley Cells, also affects the Walker Cell and causes El Niño/SOI (ENSO) events.**

14. Conclusions

The characteristics of drought in south eastern Australia: reduced rainfall; reduced humidity; and increased MSL pressure; correlate with the aerosol optical depth over the Area (10S to 10N and 90E to 160E).

Rainfall in Darfur has a statistically significant negative correlation with the aerosol index over the area to the south of Darfur and it is concluded that droughts in Darfur have been caused by the high levels of aerosols in the atmosphere over and to the south of Darfur.

Volcanic eruptions in the Area correlate negatively with rainfall in south eastern Australia over a 117 year period and the correlation of the "VEI to Tephra" data against Murray River water inflows also shows a clear negative relationship.

The scatter plots and correlations of the "VEI to Tephra" data against the Southern Oscillation Index demonstrate that volcanic aerosol plumes in the Area force the SOI to negative levels. The scatter plots and correlations of the "VEI to Tephra" data against the sea surface temperature anomalies in the Niño 3.4 region demonstrate that volcanic aerosol plumes in the Area force these SST anomalies to positive levels. It is therefore concluded that volcanic eruptions in the Area and/or the South East Asian Plume are the cause of ENSO events and it is suggested this is most likely due to the aerosol plumes interfering with the circulation of and/or moving the Walker Cell.

The conclusion that aerosol plumes in the Area cause drought in south eastern Australia is therefore inescapable.

15. Solution(s)

The solution for Australia is obvious – eliminate the anthropogenic South East Asian Plume and the climate of south eastern Australia will return to a more "normal" state within a few days as the southern Hadley Cell re-establishes its "normal" position. The major causes of the South East Asian Plume which must all be addressed are:

- Rainforest clearing - mainly for biofuels;
- Increasing levels of tropical agriculture due to increasing populations;
- Logging – both legal and illegal;
- Peat fires;
- Industrial activity.

It should be noted that the East Asian Plume may also have a role to play in climate change in south eastern Australia as it extends into the tropics to the north of Australia and will also affect the movement of the ITCZ in a way which could affect the Australian climate and this requires investigation.

The solution for Darfur is also obvious – eliminate the aerosol plume over and to the south of Darfur and the climate should return to "normal" within a few days.

And then, unfortunately of course, there will always be the volcanoes which will continue to cause droughts in south eastern Australia.

16. References

1. Intergovernmental Panel on Climate Change Fourth Assessment Report "Climate Change 2007: The Physical Science Basis. Summary for Policy Makers" at http://www.ipcc.ch/ [2007]

2. Trenberth, K.E., et al, 2007: Observations: Surface and Atmospheric Climate Change. In: Climate Change 2007: The Physical Science Basis. Contribution of Working Group I to the Fourth Assessment Report of the Intergovernmental Panel on Climate Change [Solomon, S. et al (eds.)]. Cambridge University Press, Cambridge, United Kingdom and New York, NY, USA..

3. The images used in this study were acquired using the GES-DISC Interactive Online Visualization and Analysis Infrastructure (Giovanni) as part of the NASA's Goddard Earth Sciences (GES) Data and Information Services Center (DISC). Nasa Goddard Space Flight Centre, MODIS Terra and Aqua Monthly Level-3 Data, Giovanni System at http://disc1.sci.gsfc.nasa.gov/daac-bin/G3/gui.cgi?instance_id=MODIS_DAILY_L3

4. Ramanathan, V., 2006: "Atmospheric Brown Clouds: Health, Climate and Agriculture Impacts" in the Pontifical Academy of Sciences Scripta Varia 106 Interactions Between Global Change and Human Health, (*Pontifica Academia Scientiarvm 2006***)**, pp. 47-60 at http://www-ramanathan.ucsd.edu/PASScriptaVaria106.pdf

5. Mitchell, R. M., D. M. O'Brien, and S. K. Campbell (2006), Characteristics and radiative impact of the aerosol generated by the Canberra firestorm of January 2003, *J. Geophys. Res*., **111**, D02204, doi:10.1029/2005JD006304.

6. Duncan, B. N. et al (2003), Indonesian wildfires of 1997: Impact on tropospheric chemistry, *J. Geophys. Res*., **108**(D15), 4458, doi:10.1029/2002JD003195.

7. R. A. Hansell, S. -C. Tsay, Q. Ji, K. N. Liou, and S. -C. Ou, "Surface aerosol radiative forcing derived from collocated ground-based radiometric observations during PRIDE, SAFARI, and ACE-Asia," *Appl. Opt.* **42**, 5533-5544 (2003) http://www.opticsinfobase.org/abstract.cfm?URI=ao-42-27-5533

8. World Meteorological Organization (WMO) World Radiation Data Centre at http://wrdc.mgo.rssi.ru/

9. D. O. Fuller, Kevin Murphy "The ENSO-fire dynamic in insular Southeast Asia" Dept. Geography and Regional Studies, University of Miami, Coral Gables, FL 33124 USA at http://www.as.miami.edu/geography/climatology/ClimaticChange_MS.pdf (A Condensed Version of this paper was published in *Climatic Change* (2006) 74: 435-455)

10. Global SST Anomalies. Australian Bureau of Meteorology holds the copyright for all its data and requires the following disclaimer to be included "To the maximum permitted by law, the Bureau of Meteorology excludes all liability to any person arising directly or indirectly from using this site and any information or material available from it." at http://www.bom.gov.au/bmrc/ocean/results/pastanal.htm

11. National Oceanic and Atmospheric Adnimistration at http://nomad3.ncep.noaa.gov/cgi-bin/pdisp_sst.sh

12. Australian Bureau of Meteorology holds the copyright for all its data and requires the following disclaimer to be included "To the maximum permitted by law, the Bureau of Meteorology excludes all liability to any person arising directly or indirectly from using this site and any information or material available from it." at http://www.bom.gov.au/

13. Australian Bureau of Meteorology **Monthly ENSO Wrap Up – September 2007** at http://www.bom.gov.au/

14. NASA Goddard Space Flight Centre, Global Precipitation Climatology Project Giovanni system at: http://disc2.nascom.nasa.gov/Giovanni/tovas/rain.GPCP.shtml

15. NASA Goddard Space Flight Centre, TOMS Giovanni system at http://acdisc.sci.gsfc.nasa.gov/Giovanni/toms/toms.nimbus7.shtml

16. Google Earth at: http://earth.google.com/

17. Siebert L, Simkin T (2002-). Volcanoes of the World: an Illustrated Catalog of Holocene Volcanoes and their Eruptions. Smithsonian Institution, Global Volcanism Program Digital Information Series, GVP-3, (http://www.volcano.si.edu/world/).

18. Siebert L, Simkin T (2002-). Volcanoes of the World: an Illustrated Catalog of Holocene Volcanoes and their Eruptions. Smithsonian Institution, Global Volcanism Program Digital Information Series, GVP-3, (http://www.volcano.si.edu/world/eruptioncriteria.cfm).

19. Murray Darling Basin Commission 51 Allara St, Canberra City, ACT, Australia 2601

20. National Center for Atmospheric Research in Boulder Colorado at http://www.cgd.ucar.edu/cas/catalog/climind/TNI_N34/index.html#Sec5

21. Image provided by the NOAA/ESRL Physical Sciences Division, Boulder Colorado from their Web site at http://www.cdc.noaa.gov/

22. Kalnay, E. and Coauthors, 1996: The NCEP/NCAR Reanalysis 40-year Project. *Bull. Amer. Meteor. Soc.*, **77**, 437-471.

17. Acknowledgements

I thank:

1. NASA for their free data, a superb web interface, Giovanni, to access it and exceptionally fast responses to queries from a private researcher;

2. The Smithsonian Institution for supplying their volcano database;

3. Dr O. Mayo and Mr R. Mayo for assistance with the statistics; and

4. Professor S. Greenhalgh of the University of Adelaide, Dr W. Grace of the Grace Research Network in South Australia and Dr Leon Rotstayn of CSIRO, Aspendale, Victoria, Australia for discussion and comments;

18. Funding Sources

This research project was funded personally by Keith Potts

19. Tables

	Direct Radiation J/cm^2	Diffuse Radiation J/cm^2	Global Radiation J/cm^2	
Average (< 1,000 Fires)	957	878	1,835	**Jan to July + Dec**
Average Sept & Oct	274	1135	1409	**Sept and October**
Reduction	71.4%	-29.3%	23.2%	

Table: 1 Singapore Airport Surface Radiation Data – WMO Radiation Database

Month	Correlation Coefficient	N	*P*	R^2
Aug	-0.42	8		0.18
Sep	-0.74	8	.0.05	0.55
Oct	-0.97	8	0.01	0.94
Nov	-0.96	7	0.01	0.92

Table 2: Correlation of monthly NMGS AOD and NOAA SST averaged over the Area from 2000 to 2007

	W(Tmax), km/hr		
Date	F	O	O-F
19/1	20	15	-5
20/1	20	10	-10
21/1	35	22	-13
22/1	25	15	-10
23/1	25	18	-7
24/1	20	9	-11
25/1	20	24	+4
26/1	30	24	-6

Table 3: Comparison of Forecast (F) and Observed (O) Maximum Wind Speed at the Time of Maximum Temperature at Canberra from 19 to 26 January 2003

Month	Correlation Coefficient	N	*P*	R^2
Aug	-0.72	7	0.05	0.53
Sep	-0.39	7	-	0.15
Oct	-0.91	7	0.01	0.83
Nov	-0.30	7	-	0.09

Table 4: Correlation of monthly averaged NMGS AOD over the Area and RWRD Rainfall - 2000 to 2006

Month	Correlation Coefficient	N	*P*	R^2
Aug	0.21	7	-	0.05
Sep	0.31	7	-	0.10
Oct	0.84	7	0.01	0.70
Nov	0.12	7	-	0.02

Table 5: Correlation of NMGS AOD averaged over the Area and ABOM Melbourne Airport 9:00am MSL Pressure

Month	Correlation Coefficient	N	*P*	R^2
Aug	-0.82	7	0.05	0.67
Sep	-0.89	7	0.01	0.78
Oct	-0.92	7	0.01	0.85
Nov	-0.54	7	-	0.29

Table 6: Correlation of NMGS average AOD in the Area and ABOM Swan Hill 9:00am Dew Point – 2000 to 2006

	SST in the Area	RWRD Rainfall	Swan Hill Dew Point	Melbourne Airport MSL Pressure
Aug	-0.42	-0.72	-0.82	0.21
Sep	-0.74	-0.39	-0.89	0.31
Oct	-0.97	-0.91	-0.92	0.84
Nov	-0.96	-0.30	-0.54	0.12

Table 7: Correlations of NMGS AOD over the Area 2000 to 2006/07 with characteristics of Australian drought. Green significance <0.05, Yellow significance < 0.01

	R	N	*P*	R^2
May	-0.43	14	-	
Jun	-0.35	14	-	
Jul	-0.76	14	0.01	0.58
Aug	-0.64	14	0.05	0.41
Sep	-0.28	14	-	
Oct	-0.48	14	-	

Table 8: Correlations of NGTS AI over Area D and NGGPCP Rainfall in Darfur 1979 to 1992

	A	B
Correlation	-0.20	-0.47
N	117	25
P	0.05	0.05
R^2	0.04	0.22

Table 9: Correlation of Tephra ejected by Volcanic Eruptions in the Area and ABOM rainfall in the Riverina West Rainfall District April to October
Column A: All Years 1890 to 2006 included
Column B: Only years with reported Tephra included

Correlation	-0.27
N	117
P	0.01
R^2	0.08

Table 10: Correlation of SI "VEI to Tephra" ejected by Volcanic Eruptions in the Area and ABOM rainfall in the RWRD

	All Years
Correlation	-0.18
N	116
P	0.1
R^2	0.03

Table 11: Correlation of SI "VEI to Tephra" ejected by Volcanic Eruptions in the Area and MDBC Murray River Inflows for all years from 1891 to 2006

	Averages
Correlation	-0.92
N	6.00
P	0.05
R^2	0.85

Table 12: Correlation table for segmented and averaged SI "VEI to Tephra" data and MDBC Murray River Inflows

	A	B
Correlation	-0.37	-0.93
N	7.00	6.00
P	-	0.01
R^2	0.14	0.87

Table 13: Correlation of segmented and averaged SI "VEI to Tephra" and ABOM SOI (1891 to 2006).
Column A: All years included
Column B: 1963 excluded

	A	B
Correlation	0.72	0.92
N	7.00	6.00
P	-	0.01
R^2	0.53	0.85

Table 14: Correlation of segmented and averaged SI "VEI to Tephra" and NCAR SST in Niño 3.4 region (1891 to 1999).
Column A: All years
Column B: 1963 excluded

20. Figure Legends

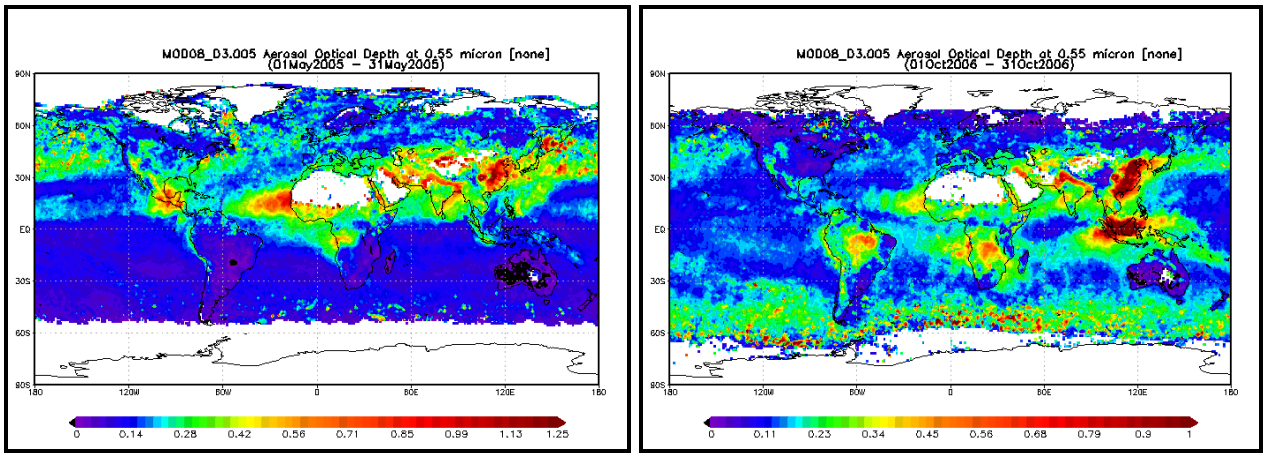

Figure 1: NMGS mean AOD images for May 2005 [L] and October 2006 [R]

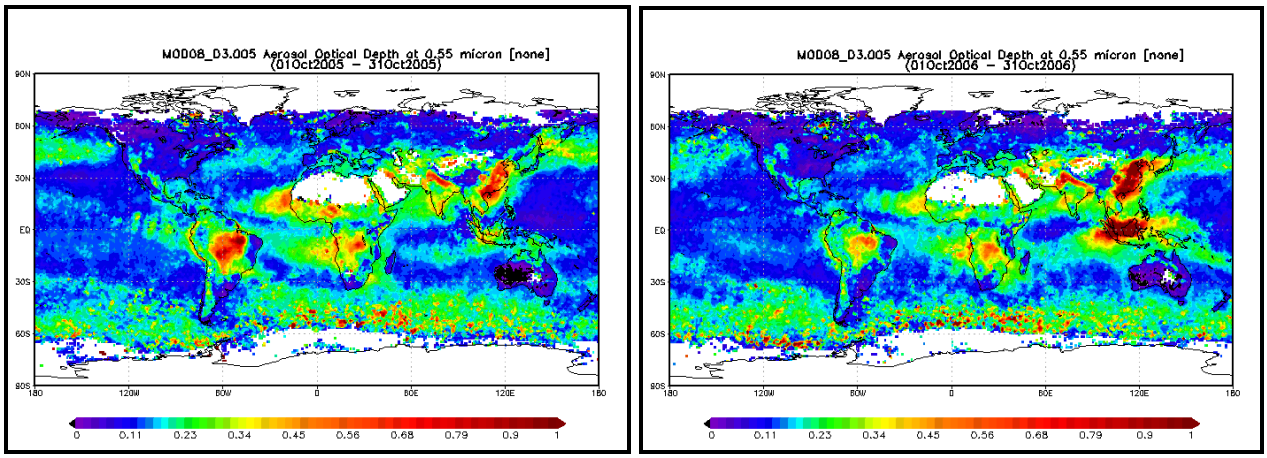

Figure 2: NMGS mean AOD Images for October 2005 [L] and October 2006 [R]

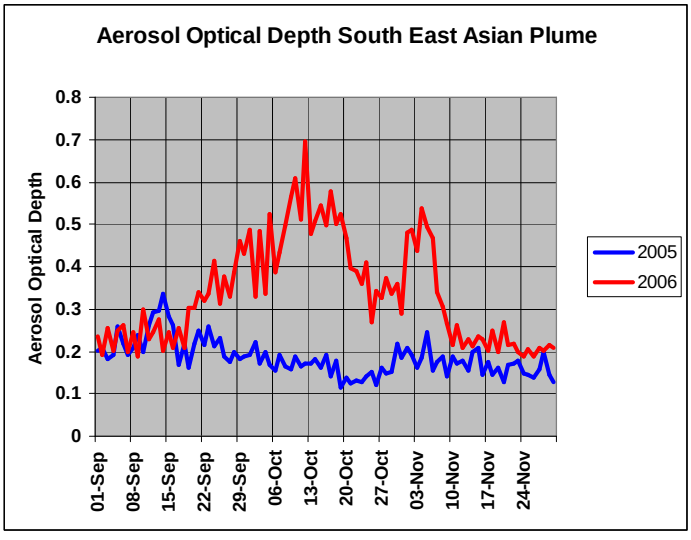

Figure 3: AOD of the South East Asian Plume September to November 2005 and 2006

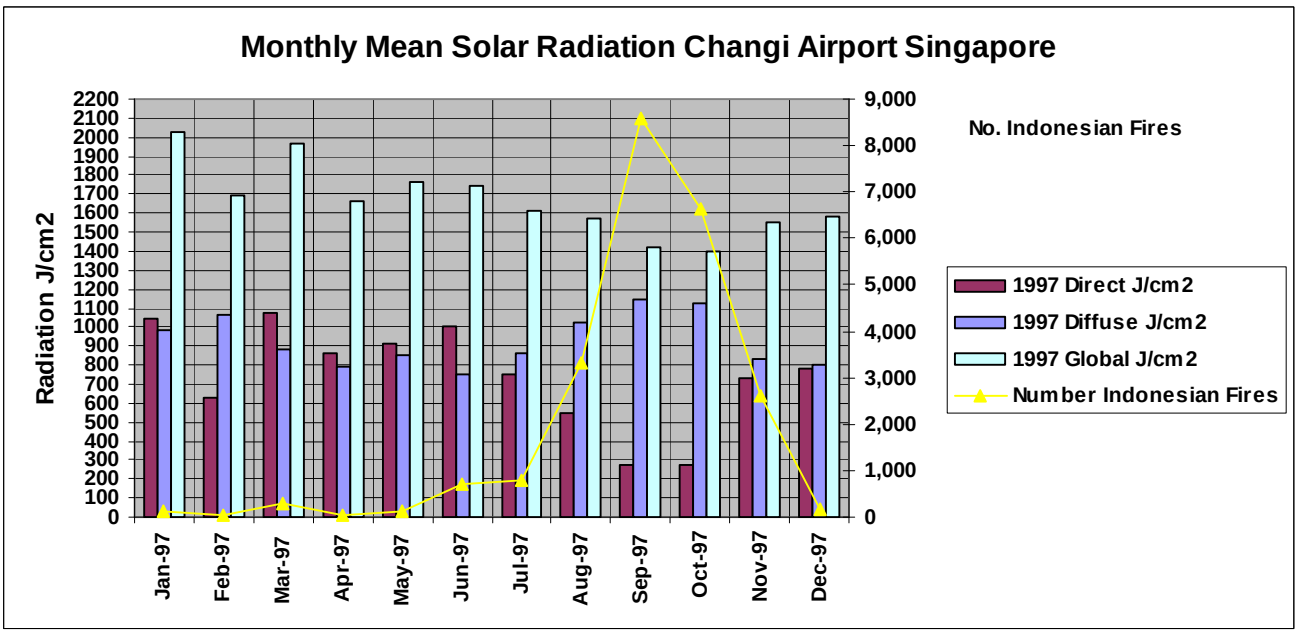

Figure 4: WMO Radiation Database mean direct, diffuse and global solar radiation at Changi Airport, Singapore during 1997 with Indonesian Fire Count

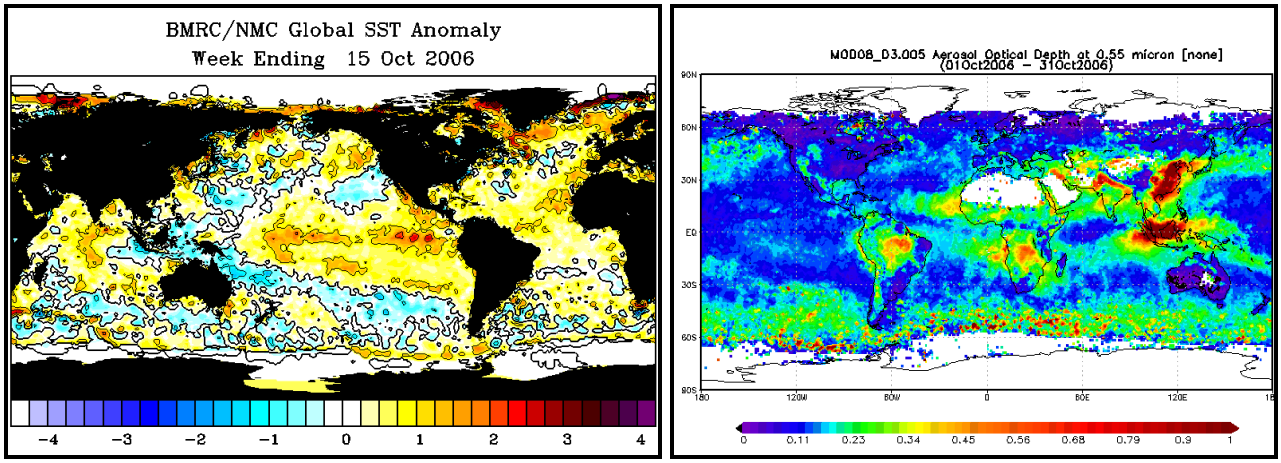

Figure 5: Sea Surface Temperature Anomalies [L] and Mean Aerosol Optical Depth October 2006 [R]

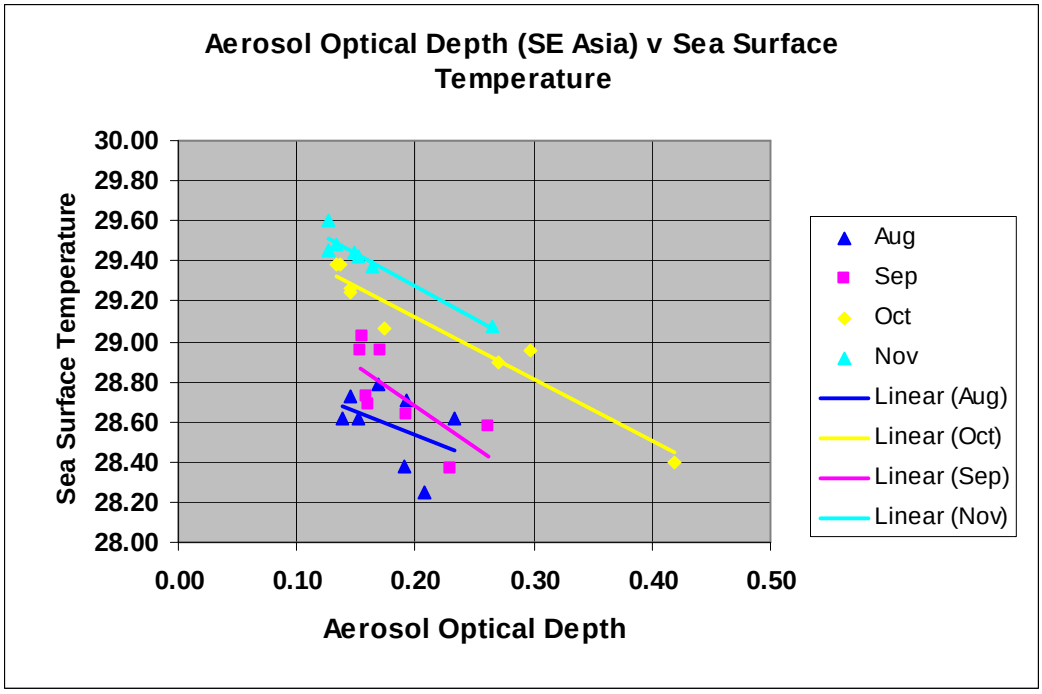

Figure 6: NOAA SST and NMGS AOD averaged over the Area for the period 2000 to 2007 with trend lines for each month

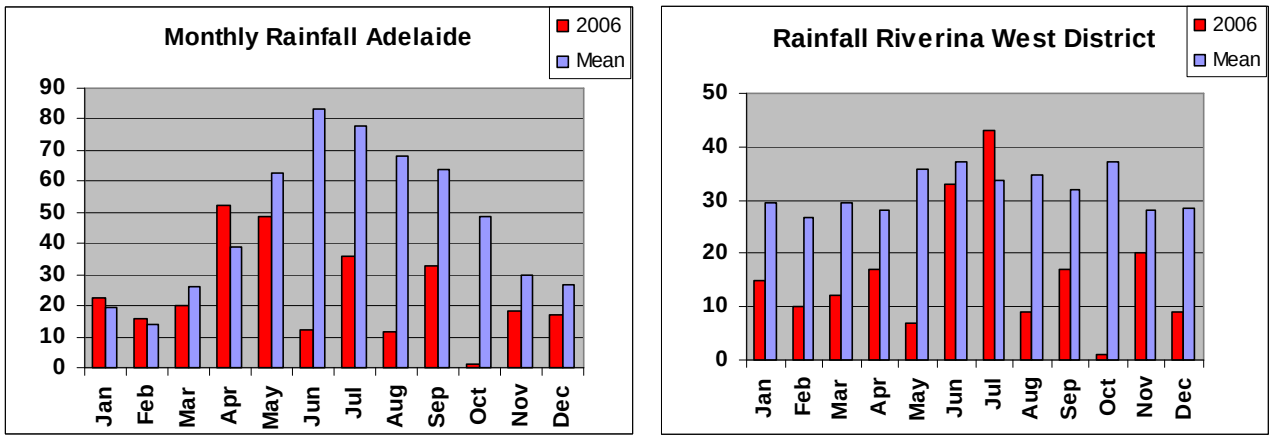

Figure 7: Mean and 2006 Monthly Rainfall in mm Adelaide and Riverina West Rainfall District

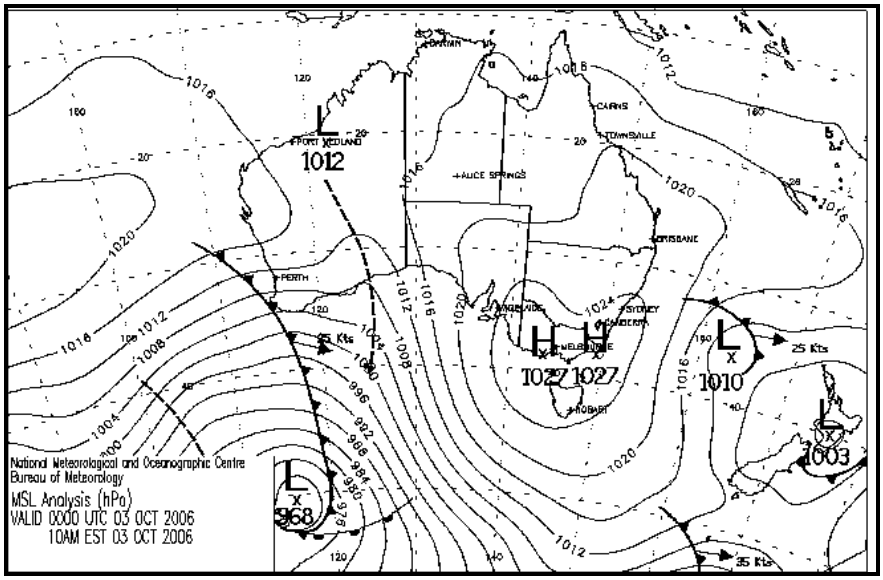

Figure 8: Australian Bureau of Meteorology MSL Analysis Chart 3rd October 2006

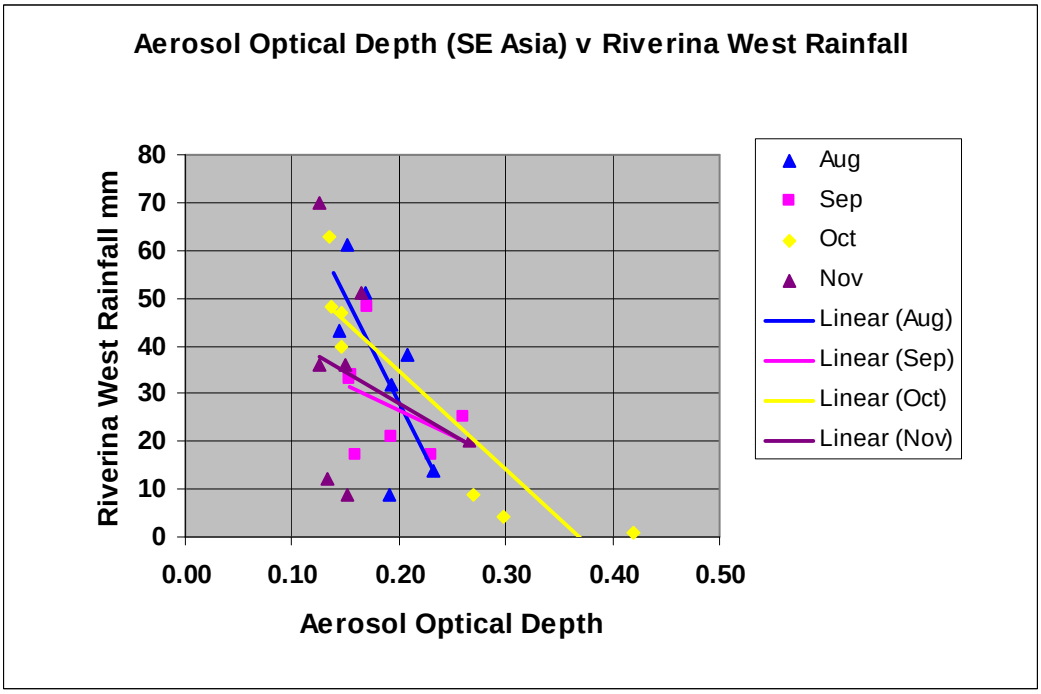

Figure 9: Scatter Plot of ABOM RWRD rainfall and NMGS AOD averaged over the Area from 2000 to 2006 with linear trend lines

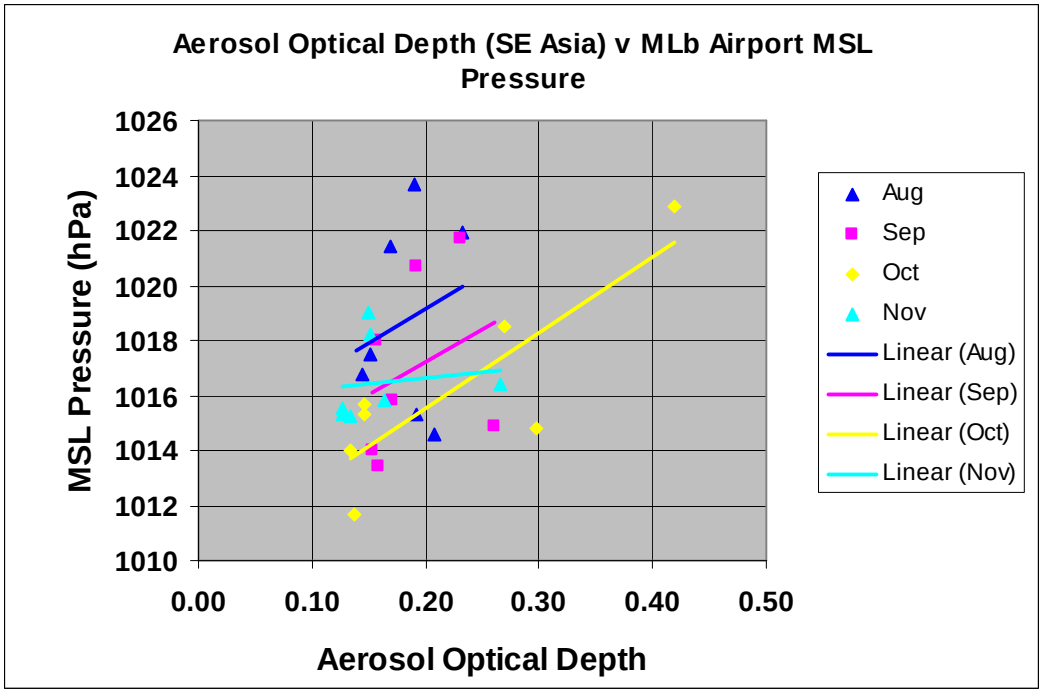

Figure 10: Scatter Plot ABOM Melbourne Airport 9:00am MSL pressure and NMGS AOD averaged over the Area from 2000 to 2006 with linear trend lines

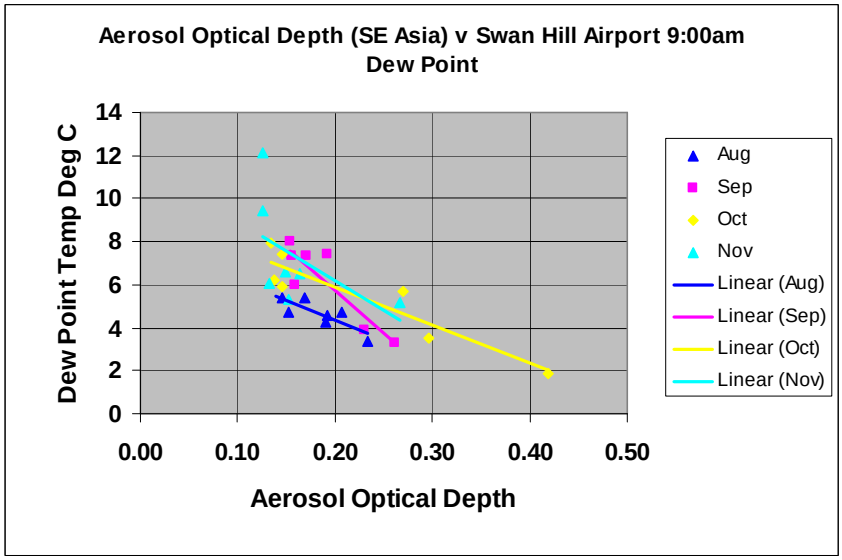

Figure 11: Scatter Plot average NMGS AOD over the Area and ABOM Swan Hill Airport 9:00am Dew Point from 2000 to 2006 with linear trend lines

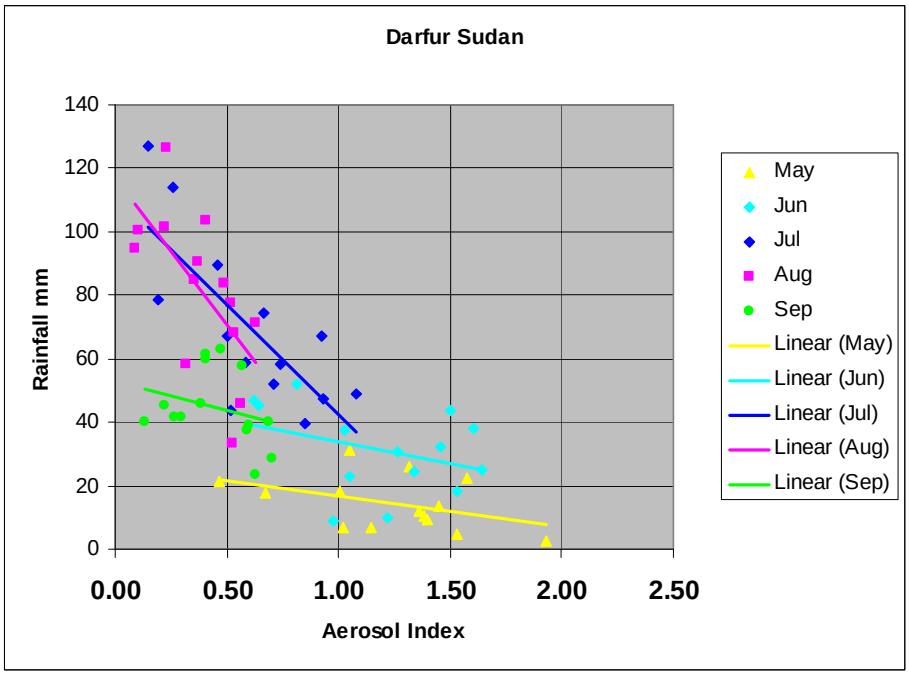

Figure 12: NGGPCP Rainfall in Darfur and NGTS AI over Area D - 1979 to 1992 with linear trend lines

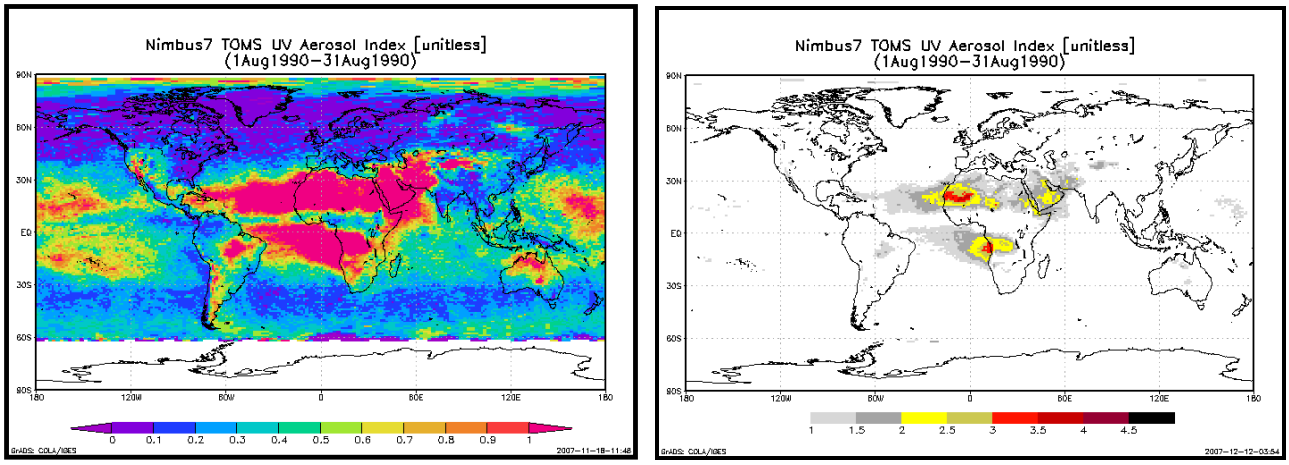

Figure 13: NGTS AI images for August 1990 using the same data and the palettes shown.

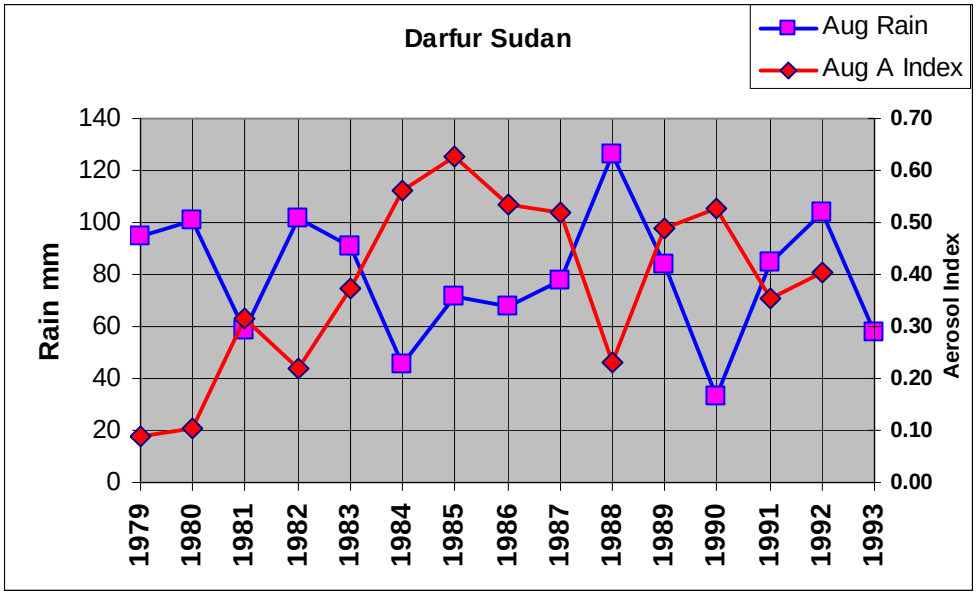

Figure 14: Plot of rainfall and aerosol index for the month of August from 1979 to 1993.

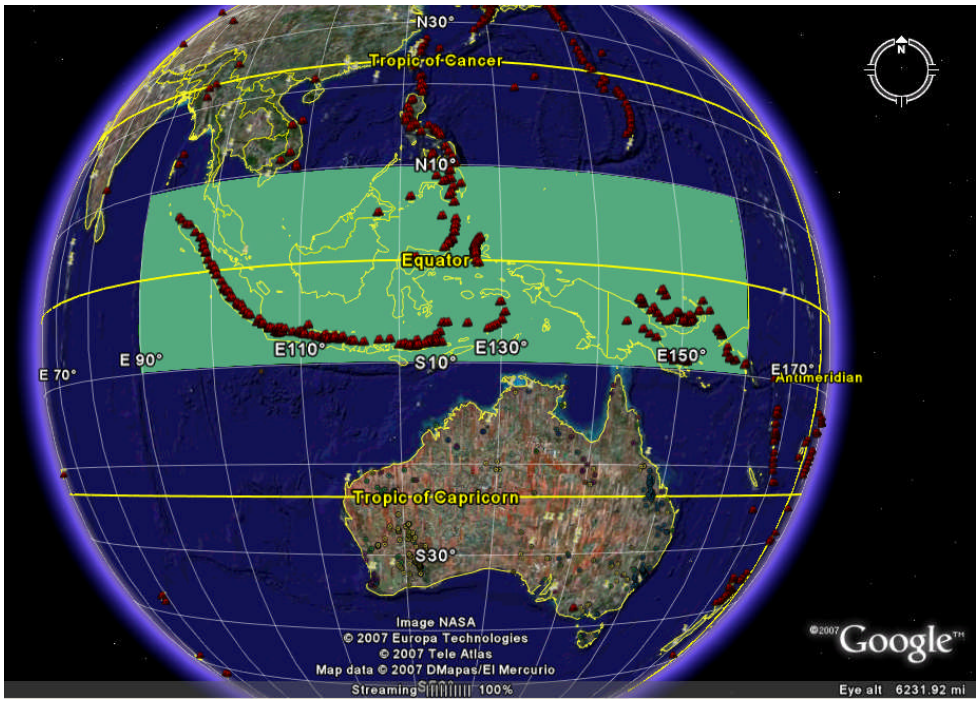

Figure 15: Google Earth with the Smithsonian Institution Volcano Overlay and the Area highlighted in pale green

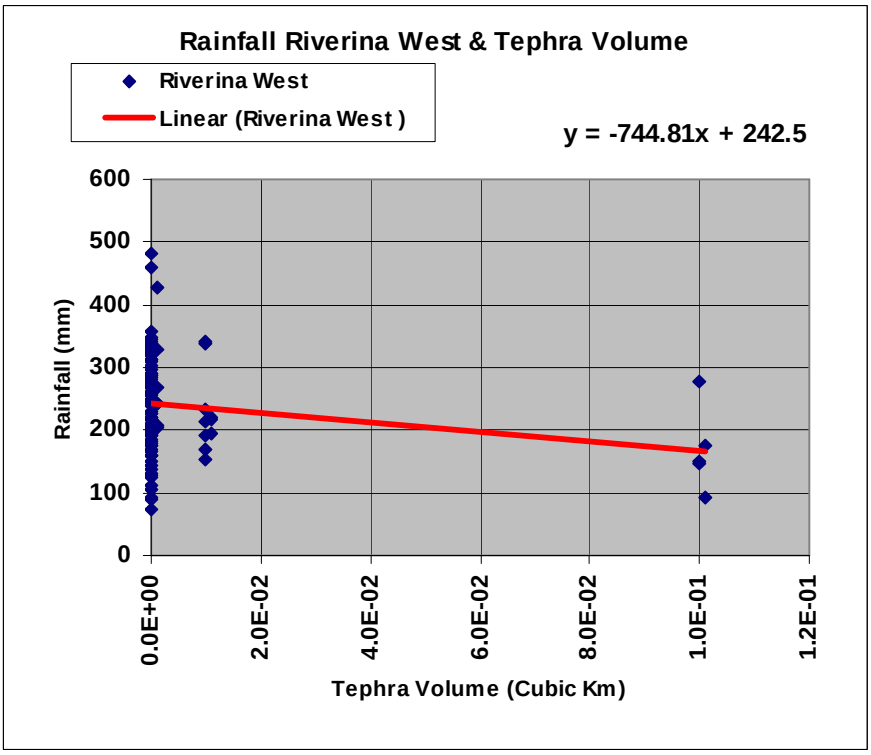

Figure 16: Scatter Plot of Riverina West Rainfall District Rainfall and Tephra ejected from Volcanoes in the area 90 to 160E and 10S to 10N for the period 1890 to 2006 with trend line

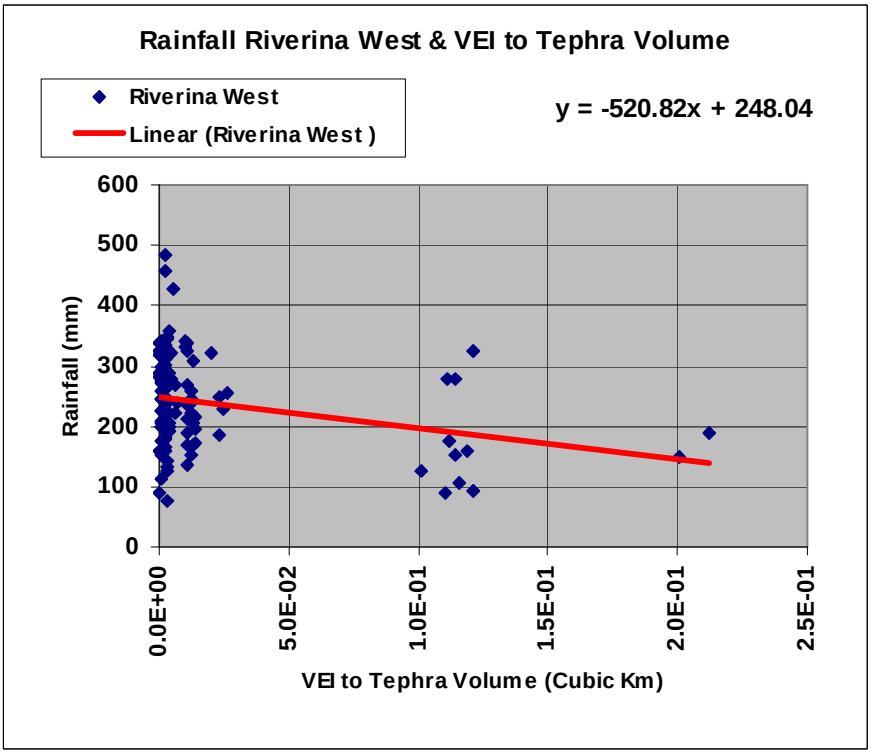

Figure 17: RWRD Rainfall and "VEI to Tephra" from Volcanoes in the Area. 1890 to 2006 with trend line

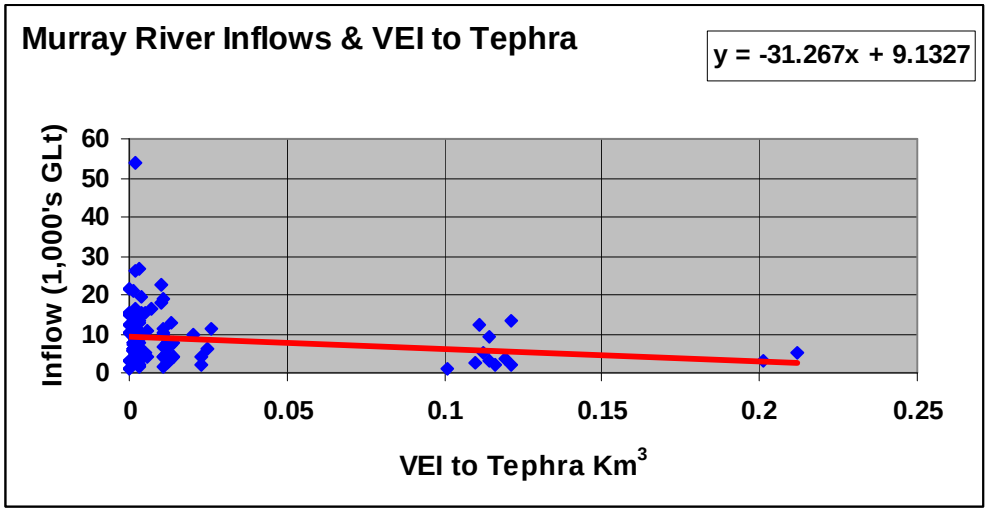

Figure 18: Murray River Inflows and "VEI to Tephra" from the Area - 1892 to 2006 with trend line

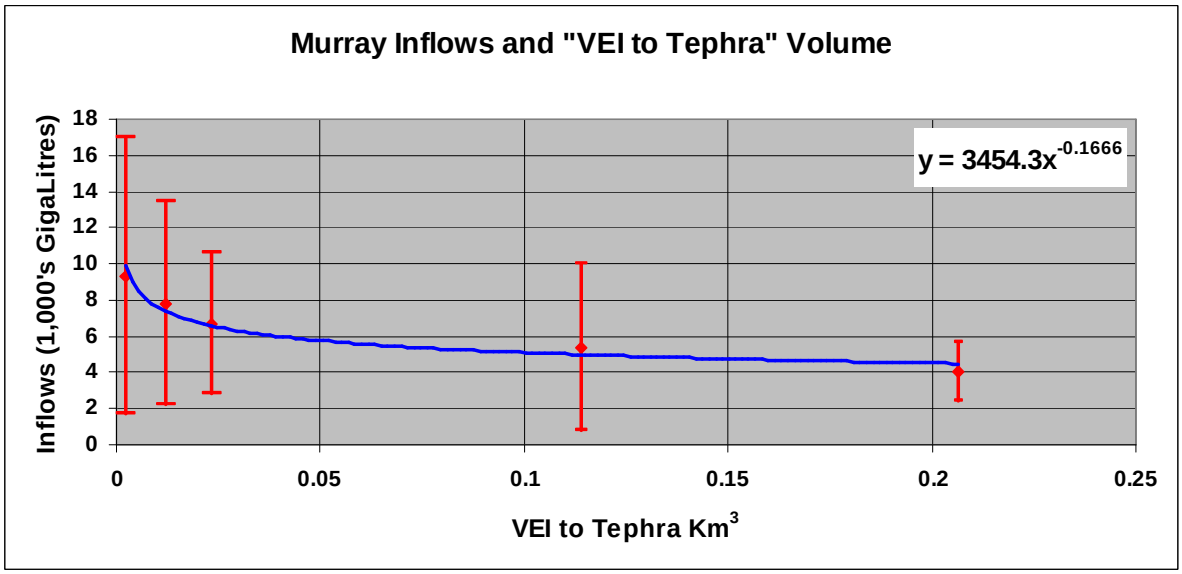

Figure 19: Scatter plot Murray River Inflows (Error Bars ± 1s.d.) and "VEI to Tephra" from the Area - 1892 to 2006 with the data segmented into "VEI to Tephra Bands" and averaged with "power" trend line.

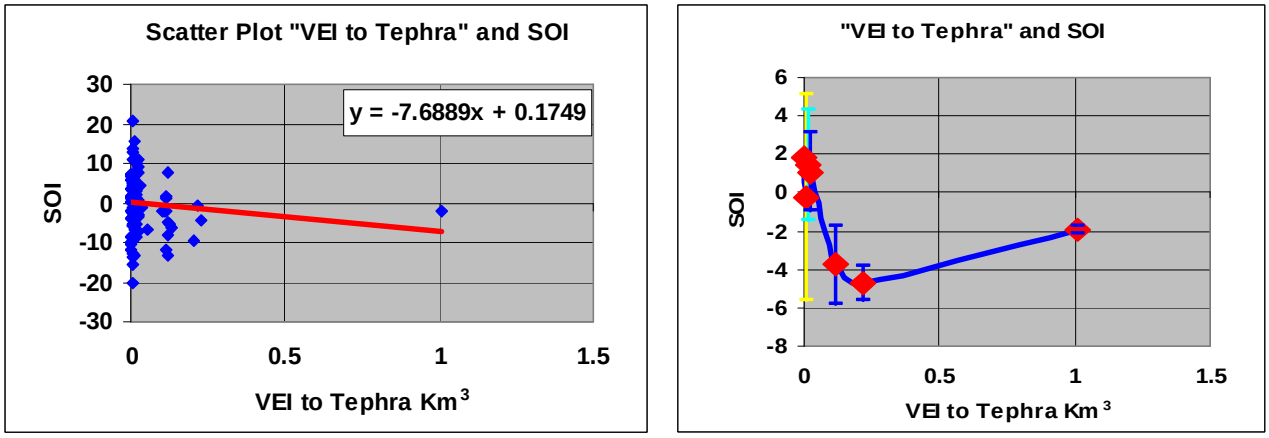

Figure 20: Scatter plots "VEI to Tephra" and SOI All Years (L) and "VEI to Tephra" and SOI ±1 s.d. Segmented and Averaged by tephra bands (R) 1891 to 2006 data for both graphs

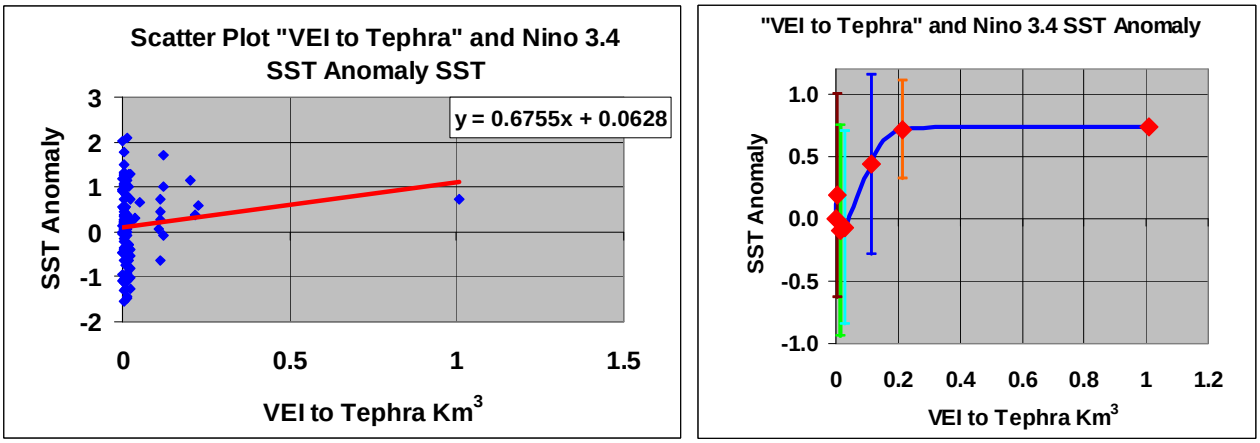

Figure 21: SI "VEI to Tephra" and NCAR SST Anomaly ^{o}C in Niño 3.4 (L) and SI "VEI to Tephra" and NCAR SST Anomaly ^{o}C ±1 s.d. in Niño 3.4 Segmented and Averaged (R) (1891 to 1999)

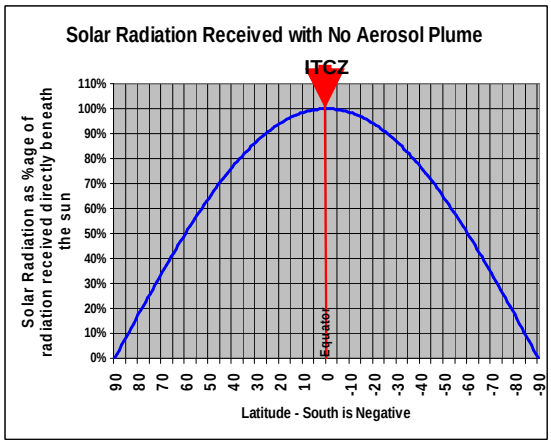

Figure 22: Solar radiation relative to maximum at the equator without an aerosol plume

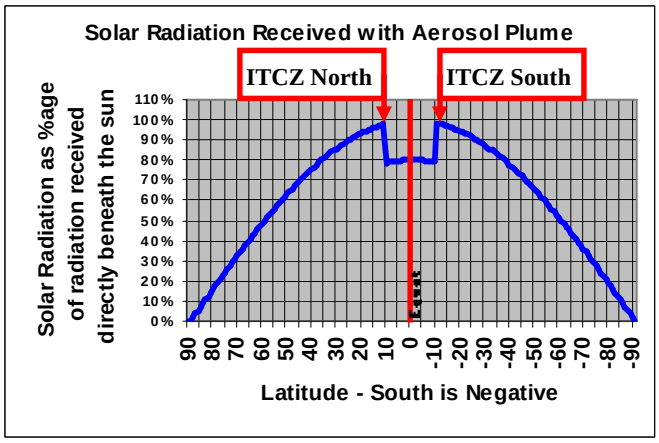

Figure 23: Surface Solar radiation relative to maximum possible at the equator with an aerosol plume 20^{o} of latitude in extent reducing solar irradiance by 20%

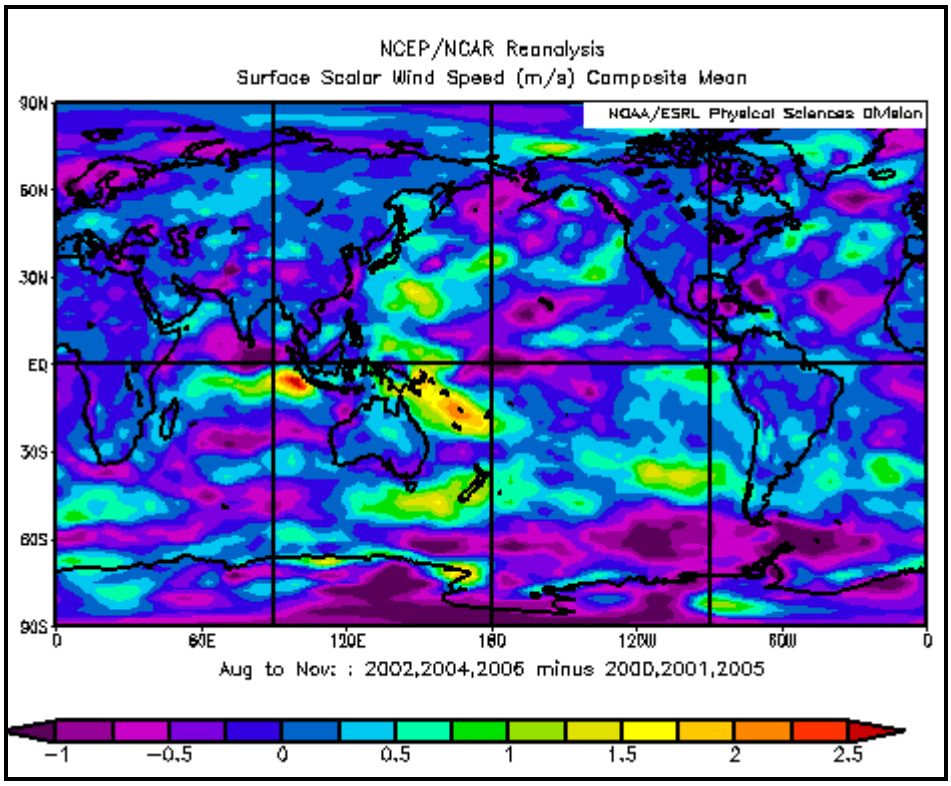

Figure 24: Surface scalar wind speed August to November. Years 2000, 2001, 2005 (Low October AOD) subtracted from 2002, 2004, 2006 (High October AOD) to show the effects of the South East Asian Plume on the wind systems